Some Characteristics of Cumulus Convection over the Tibetan Plateau

Duan Tingyang (段廷扬)
Chengdu Institute of Meteorology, Chengdu 610041, Sichuan Province
and *Elmar R. Reiter*
Center for Cybernetic Communication Research, Colorado
State University, Fort Collins, CO.80523 U. S. A.
Received March 6, 1989

ABSTRACT

The diagnostic model of the cumulus convection proposed by Yanai et al. (1973) was applied to the atmosphere over the Tibetan Plateau, and used to estimate the vertical mass flux, entrainment and detrainment, excess temperature and moisture, liquid water content, and condensation and precipitation rates of highland cloud clusters. The results illustrated that in clouds over the Tibetan Plateau, the water vapor condensation rate, liquid water content, and efficiency of the rain generation process are less than those in the tropics (represented by the Marshall Islands region). Therefore, the condensational latent heat released over the Tibetan Plateau, overall, is much smaller than that in the tropics. The water vapor and liquid water detrainment from shallow nonprecipitating cumulus clouds, and their entrainment into deep cumulus clouds, serve as a growing mechanism for the deep precipitating cumulus towers over the Tibetan Plateau. It should be noted that there is a stronger detrainment of liquid water from cumulus clouds and a stronger re-evaporation rate in environment. The process of the condensation–detrainment–re-evaporation–entrainment is repeatedly in progress. It would play an important role in maintaining of cumulus convection on the condition that the supply of moisture is not plentiful over the Tibetan Plateau.

The analyses also showed that the cloud mass flux M_c over the Tibetan Plateau is less, and the large-scale average upward motion is much less than those over the Marshall Islands. Stronger compensating downward motion in the cloud environment over the Tibetan Plateau, responsible for the area's strong environmental heating rate was revealed, and would link to the stability of the South Asian High in summer.

1. INTRODUCTION

Cumulus clud characteristics over tropical oceans and the interactions between cumulus convection and large-scale motion have been studied by many scientists (Kuo, 1965; 1974; Arakawa and Schubert, 1974; Ogura and Cho, 1973; Yanai et al., 1973; Cho, 1977; Nitta, 1975; Cho et al., 1979). These studies examined various aspects of the production and growth of tropical disturbances.

The frequent cumulus cloud activity over the Tibetan Plateau in summer and its possible influence on large-scale motion have long been an attractive subject of atmospheric circulation studies. From satellite cloud pictures, Flohn (1968) estimated cumulus cloud densities over the Tibetan Plateau to be 20 to 50 per 10^5 km^2, and stressed "the cumulus chimney effect" exerted by the huge cumulus cloud towers which transport heat to the upper troposphere. Yeh and Gao (1979) indicated that an area of highly active convective clouds occurs over the Tibetan Plateau, with typically about 300 convective cloud cells per day. Zhu et al. (1980)

explained fourther that the convective activity over the southeastern Plateau plays an important role in maintaining and building up the South Asian High. But, which characteristics of cumulus convection over the Tibetan Plateau differ from those in the tropics? Do any physical processes associated with cumulus convection over the Tibetan Plateau affect the South Asian High? These questions still remained to be answered.

Yanai et al. (1973) applied a diagnostic method to the Marshall Islands area and analyzed bulk properties of tropical cloud clusters. In the present study a similar method is used over the Tibetan Plateau, and the results are contrasted with those of the tropical atmosphere represented by the Marshall Islands area. Thus, some significant characteristics of cumulus convection over the Tibetan Plateau are revealed.

II. DATA AND COMPUTATIONS

In the method used by Yanai et al. (1973), a horizontal area large enough to contain the ensemble of clouds, but small enough to be regarded as a fraction of the large-scale system, is considered. It is assumed that:

1. In this finite area exists a variety of cloud types identified according to their different cloud top heights. Total cloud cover is very small compared to the region's total area.

2. All clouds have a common cloud base height. At a given height, the value of dry or moist static energy in clouds is the same for every cloud with the same top height.

3. Each cloud type has a thin detrainment layer at the cloud top, where the physical properties of the cloud are well mixed with those of its environment.

4. The precipitation rate is proportional to the average liquid water content, and the rate of re-evaporation is equal to the rate of liquid water detrainment.

With these assumptions, a closed set of equations for ten unknowns can be written as:

$$-M_c^{(\nu)}\frac{\partial \tilde{s}}{\partial p} = Q_1 - Q_r + L_e^{(\nu-1)} \tag{1}$$

$$\bar{h}_c^{(\nu)} - \tilde{h} = \frac{gF}{M_c^{(\nu)}} \tag{2}$$

$$\bar{s}_c^{(\nu)} - \tilde{s} = \frac{1}{1+\gamma}\left[\bar{h}_c^{(\nu)} - \tilde{h}^*\right] \tag{3}$$

$$L\left[\bar{q}_c^{(\nu)} - \tilde{q}^*\right] = \frac{\gamma}{1+\gamma}\left[\bar{h}_c^{(\nu)} - \tilde{h}^*\right] \tag{4}$$

$$\delta^{(\nu)}\left[\tilde{h}^* - \tilde{h}\right] = Q_1 - Q_2 - Q_r + M_c^{(\nu)}\frac{\partial \tilde{h}}{\partial p} \tag{5}$$

$$\varepsilon^{(\nu)} = \delta^{(\nu)} - \frac{\partial M_c^{(\nu)}}{\partial p} \tag{6}$$

$$c^{(\nu)} = \frac{\partial}{\partial p}\left[M_c^{(\nu)}\bar{q}_c^{(\nu)}\right] - \frac{\partial M_c^{(\nu)}}{\partial p}\tilde{q} - \delta^{(\nu)}\left[\tilde{q}^* - \tilde{q}\right] \tag{7}$$

$$\left[\delta^{(\nu)} + K\right]\bar{l}^{(\nu)} - \frac{\partial M_c^{(\nu)}\bar{l}^{(\nu)}}{\partial p} = c^{(\nu)} \tag{8}$$

$$r^{(\nu)} = K\bar{l}^{(\nu)} \tag{9}$$

$$e^{(\nu)} = \delta^{(\nu)}\bar{l}^{(\nu)} \tag{10}$$

where, Q_1, Q_2, Q_r, and F are the apparent heat source, apparent moisture sink, radiational heating rate and the vertical eddy flux of total heat, respectively, and can be calculated directly from synoptic-scale sounding data. $\tilde{s}, \tilde{h}$, $\tilde{h}^*$, $\tilde{q}$ and $\tilde{q}^*$ are the environmental dry, moist and saturation moist static energy, the environmental mixing ratio and saturation mixing ratio, respectively. From assumption (1), these environmental values are approximately equal to average values in this area, therefore they can also be calculated from synoptic-scale sounding data. The variable γ in the above set of equations has the form

$$\gamma = \frac{L}{C_p}\left(\frac{\partial \bar{q}^*}{\partial T}\right)_p \tag{11}$$

and can be calculated from temperature T, and pressure p. $K(p)$ is an empirical function which varies with height. In Yanai's model,

$$K(p) = \begin{cases} 60.0(p_b - p)/(p_b - p_t) & \text{in cloud} \\ 0.0 & \text{at cloud base} \end{cases} \tag{12}$$

where p_b is the pressure at the cloud base and p_t is that at cloud top. As shown in (12), $K(p)$ increases exponentially from 0.0 at cloud base to 60.0 per day (0.001 s^{-1}) in the top layer. Yanai indicated that Eq.(12) is a very crude empirical assumption, and it is necessary to examine its validity. The rate of precipitation over the Tibetan Plateau is much less than that in the tropics, so in this paper, it seems to be reasonable that the values of $K(p)$ used over the Tibetan Plateau are reduced by three times. At the cloud base, the mass flux M_{cb} and dry static energy h_{cb} can be defined by use of Yanai's method with the Bowen ratio of 76, and $\bar{l} = 0.0$ for the liquid water equation (8). Observations (Qian et al., 1984) suggest that over the Tibetan Plateau, cumulus cloud bases on the average are 1.5–2.0 km above ground level, i.e. at about 500 hPa. In this paper, therefore, the 500 hPa height is used as the height of cloud base.

In the equations, v is the index of iteration. Starting with (1), an initial guess of $e^{(0)} = 0.0$ is taken. After several iterations, the set of equations is solved, and the ten unknowns of the equations are determined. They are the mass flux M_c, average dry and moist static energy $\bar{s}_c$ and $\bar{f} = h\bar{h}_c$, average mixing ratio $\bar{q}_c$, the rates of mass entrainment and detrainment per unit pressure interval ε and δ, the rate of condensation per unit mass of air c, the cloud droplet re-evaporation rate e, the precipitation rate r, and the average liquid water mixing ratio $\bar{l}$. These solutions provide information about the cumulus cloud.

Five stations on the eastern Tibetan Plateau, Lhasa, Deqin, Ganzi, Golmud and Tuotuohe, were selected for this study. They form a pentagonal region with area $4.5 \cdot 10^5 km^2$, and an average height around 600 hPa (in this paper, the data of 600 hPa level indicate that of ground level).

The data at ground, 500, 400, 300, 250, 200, 150, and 100 hPa levels of 0000 and 1200 GMT between 1 June and 31 August 1983 were used for these calculations. They were obtained from the "Monthly Aerological Bulletin of China". The humidity above 150 hPa was linearly extrapolated from those below 150 hPa. The radiative heating rate Q_r was a climatological vertical profile taken from Katayama (1967).

III. LARGE-SCALE MASS, HEAT AND MOISTURE BUDGETS

1. *Divergence and Vertical Velocity*

The area-averaged horizontal divergence over the pentagonal region was computed using

$$\overline{\nabla \cdot \mathbf{V}} = \frac{1}{S}\left[\sum_{i=1}^{5} V_{ni} L_i\right] \tag{13}$$

where S is the area of the pentagon, L_i is the length of pentagonal side i, and V_{ni} is the wind component perpendicular to the pentagon boundary. The average vertical p-velocity is

$$\overline{\omega} = \int_{P_0}^{P} \overline{\nabla \cdot \mathbf{V}} dp \tag{14}$$

Because of the forcing effect of the underlying surface, the vertical velocity ω at the surface must be calculated. Slight corrections to the original divergence estimated by use of O'Brien's method were added to make ω vanish at 100 hPa.

The vertical profile of the average horizontal divergence is shown in Fig.1 (solid). An intense but shallow convergence layer appears from the surface to 400 hPa, with a deep divergence layer aloft. Maximum convergence occurs at the surface due to boundary layer friction and the frequent low pressure systems moving through this layer. The maximum divergence is found at 200 hPa, where the south Asian High, situated over the Tibetan Plateau during summer, is strongest.

The corresponding vertical p-velocity is illustrated in Fig.1 (dashed). An average upward motion consistently appears over the Tibetan Plateau in summer, with a maximum of 1.3 hPa / hour at 400 hPa. This maximum is smaller than the 4 hPa / hour obtained by Yanai et al. (1973) for the tropical atmosphere

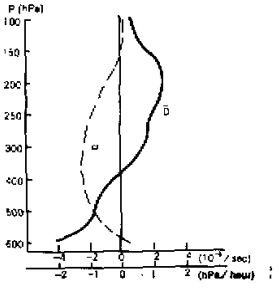

Fig.1. The mean horizontal divergence (solid) and vertical p-velocity (dashed).

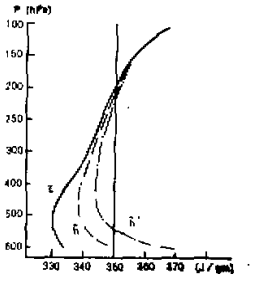

Fig.2. The mean dry static energy $\bar{s}$ (solid), moist static energy $\bar{h}$ (dashed), and saturation moist static energy $\bar{h}^*$ (dash-dotted) of the environment.

2. *Static Energy*

The area-averaged dry and moist static energy were obtained using

$$\bar{s} = C_p \bar{T} + g\bar{z} \tag{15}$$

$$\bar{h} = C_p \bar{T} + g\bar{z} + L\bar{q} \tag{16}$$

The saturation moist static energy $\bar{h}^*$ is determined using Eq.(16) by replacing $\bar{q}$ with the saturation mixing ratio $\bar{q}^*$. These area-averaged values may be equated approximately with the environmental values.

The mean vertical profile of the dry static energy $\tilde{s}$, the moist static energy $\tilde{h}$, and its saturation value $\tilde{h}^*$ are shown in Fig.2. Both $\tilde{s}$ and $\tilde{h}$ reach their minimum at 500 hPa. Below 500 hPa, $\tilde{h}$ is much larger than $\bar{s}$. The atmosphere is clearly unstable due to its high temperature and high humidity in low levels though there probably is a mixed layer near the surface. In the upper troposphere $\tilde{h}$ approaches $\tilde{s}$ and the distinction between the two curves becomes negligible above 200 hPa. The saturation value $\tilde{h}^*$ is very large compared with $\tilde{h}$ in the lower troposphere, is markedly constant between 500 and 250 hPa, and is equal to $\tilde{h}$ above the 200 hPa level.

The vertical distribution of static energy in the highland atmosphere differs greatly from the results of tropical atmosphere (Yanai et al., 1973). The major differences are:

i. In the tropical region, the dry static energy increases with height from its minimum at the sea surface. Over the Tibetan Plateau, however, the dry static energy initially decreases with height above the surface to its minimum at 500 hPa, and then it increases with height. This means that there is an intense sensible heat transfer from the highland surface to the air.

ii. The values of the dry, moist and saturation static energy at all heights over the Tibetan Plateau are much larger than those at the same heights over the tropical ocean. This is because the Tibetan Plateau is a huge high-altitude heat source which directly transports sensible heat and moisture to the atmosphere above.

iii. Between 500 and 100 hPa, the vertical gradients of the three curves in the highland atmosphere are larger than those for the tropical atmosphere. The highland atmosphere is relatively stable compared to the tropical atmosphere above the 500 hPa level.

iv. In the tropical area, $\tilde{h}$ is close to $\tilde{h}^*$, and larger than $\tilde{s}$ at lower levels; in the Plateau area, however, $\tilde{h}$ is fairly close to $\tilde{s}$. This means that the supply of moisture is not plentiful in the Tibetan Plateau atmosphere.

These different atmospheric features seriously affect the cumulus convection in these two areas.

3. *Apparent Heat Source and Moisture Sink*

The heating rate due to the apparent heat source Q_1 is given by

$$\frac{Q_1}{C_p} = \frac{1}{C_p}\left[\frac{\partial \bar{s}}{\partial t} + \overline{\nabla \cdot s\mathbf{V}} + \frac{\partial \overline{s\omega}}{\partial p}\right] \tag{17}$$

The equivalent heating rate due to the apparent moisture sink Q_2 is

$$\frac{Q_2}{C_p} = -\frac{L}{C_p}\left[\frac{\partial \bar{q}}{\partial t} + \overline{\nabla \cdot q\mathbf{V}} + \frac{\partial \overline{q\omega}}{\partial p}\right] \tag{18}$$

The time–averaged vertical profiles of Q_1 and Q_2 are illustrated in Fig.3. Both Q_1 and Q_2 are expressed in units of heating rate (℃ / d). At the surface Q_2 is a small negative, and Q_1, produced by the transfer of sensible heat from the surface to the air, is 2.4℃ / d. Q_1 reaches its maximum (4.3℃ / d) at 400 hPa. This maximun is very close to 5℃ / d between 300 and 400 hPa over the eastern Plateau obtained by Luo and Yanai (1984). Below 200 hPa Q_2 is quite small and, at some levels, even less than half of Q_1. This difference between the Plateau atmosphere and the tropical atmosphere is noteworthy. The highland atmosphere's heating depends both on the release of condensation latent heat and on the upward transfer of sensible heat from the surface, but not chiefly on the release of the condensation latent heat. This fact was also noted by Chen et al. (1985a) and Chen et al. (1985b). Q_2 has the maximum at a much lower level, namely at 500 hPa. This suggests that a lot of shallow cumulus clouds surround the deep cumulus towers above the Tibetan Plateau. This conclusion was confirmed by the observations of the radar echo around Nagqa (Qin et al. 1984).

The climatological radiative heating rate Q_r is shown on the left side of Fig.3.

With the vertical profiles of Q_1, Q_2 and Q_r, the required vertical flux of eddy heat transport may be computed using

$$F = -\frac{1}{g}\overline{h'\omega'} = \frac{1}{g}\int_{P_t}^{P} (Q_1 - Q_2 - Q_r)dp \tag{19}$$

where P_t is the pressure at cloud top. The flux is assumed to be zero at the 100 hPa level near the tropopause. An upward vertical eddy heat flux consistently appears in the troposphere, which decreases with height from its maximum of 964 J $cm^{-2}d^{-1}$ at the surface to zero near the tropopause.

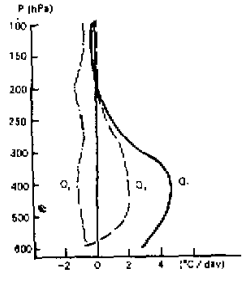

Fig.3. The mean apparent heat source Q_1 (solid) and moisture sink Q_2 (dashed). On the left is the radiational heating rate Q_r (dash–dotted) given by Katayama (1967).

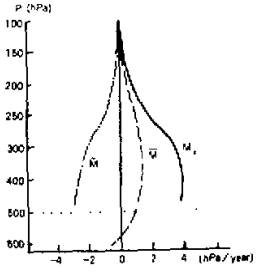

Fig.4. The average cloud mass flux M_c (solid), large–scale mass flux $\bar{M}$ (dashed), and residual mass flux $\tilde{M}$ (dash–dotted).

IV. AVERAGE PROPERTIES OF CUMULUS ENSEMBLES

Equations (1)–(10) were applied to 184 cases (two cases per day from 1 June to 31 August, 1983). The iteration converged for 126 cases. In them, 82 cases are at 1200 GMT and only 44 cases are at 0000 GMT. In the following, only the time– averaged vertical distributions

of the 126 samples are shown.

1. *Cloud Mass Flux*

The average vertical profiles of the cloud mass flux M_c, the large-scale mean mass flux $\overline{M} = -\overline{\omega}$, and the residual mass flux in the environment, $\tilde{M} = \overline{M} - M_c$, are shown in Fig.4. Similar to the tropical atmosphere, M_c exceeds $\overline{M}$ at every level, i.e., the upward mass flux in active cumulus clouds is larger than the mass flux required from the large-scale horizontal convergence. This suggests that the residual mass flux is generally directed downward. This sinking motion warms the environment by adiabatic compression. A stronger sinking motion, i.e., a stronger heating of the environment by adiabatic compression, occurs between 500–300 hPa levels over the Plateau area. This is because, though the cloud mass flux M_c is less than, yet the large-scale mean vertical mass flux $\overline{M}$ is even less than that of the tropical atmosphere above 600 hPa level.

2. *Entrainment and Detrainment*

Fig.5 shows the average vertical distribution of entrainment and detrainment. Because a variety of cloud types coexists, entrainment ε and detrainment δ take place at the same height. At the lowest level, entrainment is greater than detrainment and both are at a maximum. The detrainment maximum must be the result of a large number of shallow clouds detraining immediately from their low cloud tops. Both entrainment and detrainment rapidly decrease with height. Entrainment approaches zero above 300 hPa. Detrainment, however, increases at 250 hPa and reaches a secondary maximum at 200 hPa, where the deep cumulus clouds have their top layers. By analyzing the stratification curves, Qian et al. (1984) estimated that, in practice, the average convective cloud top height can reach 200 hpa or even higher over the eastern Plateau in the rainy season.

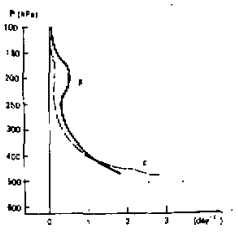

Fig.5. The average detrainment δ (solid) and entrainment ε (dashed).

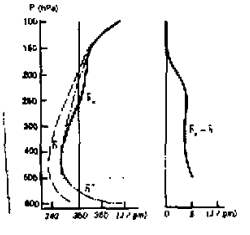

Fig.6. Left: The average moist static energy of the cloud ensembles $\overline{h}_c$ (solid), compared with the moist static energy $\tilde{h}$ (dashed) and saturation moist static energy $\tilde{h}^*$ (dash-dotted) of the environment. Right: Excess moist static energy of the cloud ensembles.

3. *Moist Static Energy of Clouds*

The mean vertical profile of the moist static energy of the cloud ensemble $\bar{h}_c$ is shown in Fig.6 (left) together with the average profiles of $\tilde{h}$ and $\tilde{h}^*$. Near the cloud base, $\bar{h}_c$ is almost equal to $\tilde{h}^*$, the saturation static energy of the environment; thus, the cloud has practically zero buoyancy. The average $\bar{h}_c$ increases with height more rapidly than does the environmental saturation static energy.

The excess static energy ($\bar{h}_c - \tilde{h}$) is shown in Fig.6 (right). Its maximum, 5.2 J / gm, occurs near cloud base.

4. *Cloud Temperature, Moisture and Liquid Water Content*

In Fig.7, the average profiles of the excess temperature ($\bar{T}_c - \tilde{T}$), the excess mixing ratio ($\bar{q}_c - \tilde{q}$), and the liquid water content $\bar{l}$ of the cloud ensemble are shown.

Near cloud base the cloud temperature is 0.2℃ lower than that in the environment. The excess temperature of the cloud increases rapidly with height, and the cloud temperature is higher than that of the environment above 450 hPa. In particular, from 300 hPa to 250 hPa, where entrainment and detrainment are very weak, the excess temperature reaches its maximum (0.6℃). Following the vertical mass transfer, sensible heat and latent heat are transported to upper cloud layers, warming the upper troposphere.

The excess mixing ratio gradually decreases with height, vanishing above 200 hPa, where both the cloud and the environment are very dry. Its maximum, 1.4 gm / kg, occurs near cloud base.

Most of the cloud liquid water is below 300 hPa. Its maximum is 1.5 gm / kg at 400 hPa, less than the 2.0 gm / kg maximum for the tropical atmosphere.

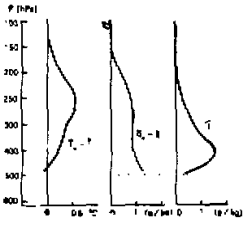

Fig.7. The average excess temperature, excess mixing ratio and liquid water content of the cloud ensembles.

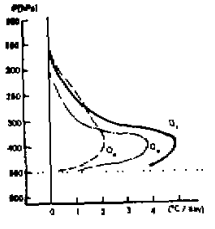

Fig.8. The average rates of condensation Q_c (solid), precipitation Q_p (dashed), and re-evaporation Q_e (dash-dotted) in equivalent heating units.

5. *Condensation, Precipitation and Re-evaporation*

In Fig.8, the vertical distribution of the mean rates of condensation, precipitation and evaporation in clouds is shown in equivalent heating units. Cloud condensation mainly occurs below 200 hPa, with a maximum at 400 hPa, where the latent heat of condensation can make air temperature rise by 4.9℃ per day. The precipitation rate reaches its maximum at 400 hPa. At lower levels, the precipitation rate is much smaller than the condensation rate, therefore, clouds have re–evaporated. The re–evaporation rate is even larger than the precipitation at 400 hPa. The efficiency of the rain generation process (the ratio of total precipitation to total condensation) is 41%, much less than that for the tropical area (84%). In fact, the low efficiency of the rain generation process is one reason why the accumulated precipitation over the Tibetan Plateau is so small.

6. *Environmental Heat and Moisture Balance*

If the detrainment of sensible heat from the clouds to the environment is neglected, except in the uppermost layer, as shown in Eq. (1), the heat source $(Q_1 - Q_2)$ can be expressed as the sum of the adiabatic heating due to the compensating downward motion in the environment $-M_c(\partial\bar{s}/\partial p)$, and the cooling due to cloud droplet evaporation $-Le$. The cooling effect of cloud droplet evaporation is small and only contributes appreciably at lower levels. Therefore, the environmental heating is mainly due to the adiabatic heating from the compensating downward motion.

Equations (1), (5) and (10) may produce

$$-\frac{Q_2}{L} = -M_c\frac{\partial\bar{q}}{\partial p} + \delta[\bar{q}_c - \bar{q}] + \delta\bar{l} \tag{20}$$

The apparent moisture sink (Q_2) is primarily caused by the induced downward motion $(-M_c)$. This alone would dry out the environmental air; however, the detrainment of water vapor and liquid water from the clouds provides environmental moisture. As mentioned above, strong detrainment occurs at low levels due to the large number of shallow clouds. This implies that the shallower, non–precipitating cumulus clouds are needed to sustain the growth of deep, precipitating cumulus clouds by supplying moisture. It is quite evident that, the process of the condensation of water vapor in clouds, the detrainment of liquid water, the re–evaporation of the detrainmental liquid water in environment, and then, entrainment to clouds is repeatedly in progress. It would play an important role in maintaining of cumulus convection on the condition that the supply of moisture is not plentiful over the Tibetan Plateau.

V. CONCLUSION

In this paper, large–scale heat and moisture budgets have been analyzed. Furthermore, some properties of Tibetan Plateau cloud clusters have been illustrated via diagnosis. The major conclusions of this study are as follows:

The cloud mass flux exceeds the mean vertical mass flux required by the large–scale convergence, thus causing a compensating sinking motion between active clouds. The large–scale heating of environmental air is primarily due to its adiabatic compression in the compensating downward motion. Detrainment of water vapor and liquid water from the shallow clouds at lower levels made up for the drying due to the environmental sinking motion. Thus, through the entrainment and vertical transfer of water vapor, shallow, non–

precipitating cumulus clouds support the growth of deep, precipitating cumulus towers. These interactions between cumulus convection and the large-scale environment are very simlar to the results obtained by Yanai et al. (1973) over a tropical ocean.

Cumulus convection over the Tibetan Plateau differs from that over the tropical Marshall Islands because of their different geographical locations, different surface features and special topographical effects. (A), Over the Tibetan Plateau there is no abundant moisture supply. Therefore, the condensational ratio is lower, the cloud liquid water content is less and the efficiency of the rain generation process is lower than in the tropics. As the result, the large-scale condensational latent heating release over the Tibetan Plateau is much less than that for the Marshall Islands. It should be noted, however, that a large amount of sensible heat energy is transported from the highland surface to the air. Due to entrainment and vertical mass transfer, sensible heat and latent heat are transported to high cloud levels; (B), Over the Tibetan Plateau, there is a stronger detrainment of liquid water from cumulus clouds. The re-evaporated rate in environment is even larger than the precipitation below 400 hPa level. The moistened environmental air is entrained in clouds, and supports the growth of cumulus convection. The process of the condensation-detrainment-re-evaporation-entrainment is repeatedly in progress. It would play an important role in maintaining of cumulus convection on the condition that the supply of moisture is not plentiful over the Tibetan Plateau; (C), Though the cloud mass flux M_c over the Tibetan Plateau is less, yet the large-scale average upward motion is much less than over the Marshall Islands. Certainly, a stronger compensating downward motion appears in the environment. Due to adiabatic compression, the heating of the large-scale environment over the Tibetan Plateau is stronger than that of the upper levels of the tropical troposphere. The stability of the South Asia high above the Tibetan Plateau in summer would be associated with this intense heating.

In this study, only the time-averaged vertical distributions of cloud cluster parameters were considered. Questions concerning the evolution of cumulus convection with time, and its relation to the activity of the South Asia high remain to be further investigated.

We thank professors Chen Longxun, Zhu Fukang and Li Weiliang for many helpful suggestions throughout the research. The assistance of Mr. Hu Qi and Mrs. Marjorrie Klitch in writing this paper is gratefully acknowledged.

REFERENCES

Arakawa, A. and W. H. Schubert, (1974), Interaction of a cumulus cloud ensemble with the large-scale environment, Part I. *J.Atmos. Sci.*, **31:** 674-701.

Chen, L. X., E. R. Reiter and Z. Q. Feng, (1985a), The atmospheric heat source over the Tibetan Plateau: May-August 1979, *Mon. Wea. Rev.*, **113:** 1771-1790.

--,T.Y. Duan and W.L. Li, (1985b), The variation of atmospheric heat source and the budget of atmospheric energy over the Qinghai-Xizang Plateau during summer 1979, Acta Meteor. Sinica, 43(1) (in Chinese).

Cho, H.R., (1977), Contributions of cumulus cloud life-cycle effects to the large-scale heat and moisture budget equations, *J. Atmos. Sci.* **34:** 87-97.

--, L. Cheng and R.M. Bloxam, (1979), The representation of cumulus cloud effects in the large-scale vorticity equation, *J. Atmos. Sci.*, **36:** 127-139.

Flohn, H., (1968), Contributions to a meteorology of the Tibetan Highlands, *Atmos. Sci. Paper*, No. 130, Atmospheric Science Department, Colorado State University, Fort Collins, CO 80523. 120 pp.

Katayama, A., (1967), On the radiation budget of the troposphere over the northern hemisphere (iii), *J. Meteor. Soc. Japan*, **45:** 26-38.

Kuo, H. L., (1965), On formation and intensification of tropical cyclones through latent heat release by cumulus convection, *J. Atmos. Sci.*, **22:** 40-63.

—, (1974), Further studies of the parameterization of the influence of cumulus convection on large-scale flow, *J. Atmos. Sci.*, **31**: 1232–1240.

Luo, H. B. and M. Yanai, (1984), The large-scale circulation and heat sources over the Tibetan Plateau and surrounding areas during the early summer of 1979, Part II: Heat and moisture budgets, *Mon. Wea. Rev.*, **112**: 966–989.

Nitta, T., (1975), *Observational determination of cloud mass flux distributions*, *J. Atmos. Sci.*, **32**: 73–91.

Ogura, Y.and H.R. Cho, (1973), Diagnostic determination of cumulus cloud populations from observed large-scale variables, *J. Atmos. Sci.*, **30**: 1276–1286.

Qian, Z. A., S. M. Zhang and F. M. Shan, (1984), The analyzes of the convective cloud in the Tibetan area during summer 1979. *The collected papers of QXPMEX (1)*, Science Press, Beijing, 243–257.

Qin, H. D., H. S. Zhou, J. X. Liu, X.R. Yang and Z. Qu, (1984), The *statistical features of the convective precipitation* echo in Nagqa area of the Tibetan Plateau, *The collected papers of QXPMEX (1)*, Science Press, Beijing, 258–268.

Yanai, M., S. Esbensen and J. H. Chu, (1973), Determination of bulk properties of tropical cloud clusters from large-scale heat and moisture budgets, *J. Atmo. Sci.*, **30**: 611–627.

Yeh, T. C. and Y. X. Gao, (1979), *The meteorology of the Qinghai–Xizang Plateau*, Science Press, Beijing 278 pp. (in Chinese).

Zhu, F. K., L. H. Lu, X. G. Chen and W. Zhao, (1980), *The South Asian High*, Science Press, Beijing, 95 pp. (in Chinese).

LIST OF SYMBOLS

C_p Specific heat at constant pressure of dry air
K Empirical function
L_i Lengths of the pentagonal sides
$\tilde{M}$ Residual mass flux in environment
Q_1 Apparent heat source
Q_c Rate of condensation in equivalent heating unit
Q_p Rate of precipitation in equivalent heating unit
S Area of the pentagonal region
$\bar{V}$ Horizontal wind
c Rate of condensation per unit mass of air
g Gravitational acceleration
$\bar{h}^*$ Regional averaged saturation moist static energy
$\tilde{h}^*$ Environmental saturation moist static energy
h' Departure from the time mean of moist static energy
p Pressure
p_b Pressure at the cloud base
$\bar{q}$ Regional averaged mixing ratio
$\tilde{q}$ Environmental mixing ratio
$\bar{q}_c$ Cloud mixing ratio
$\bar{s}$ Regional averaged dry static energy
$\bar{s}_c$ Cloud dry static energy
ν Index of iteration
δ Rate of mass detrainment per unit pressure interval
ω Vertical p-velocity
ω' Departure from the time mean of vertical p-velocity
F Vertical eddy flux of total heat
L Latent heat of condensation
$\bar{M}$ Large-scale mean mass flux
M_c Cloud mass flux
Q_2 Apparent moisture sink
Q_e Rate of re-evaporation in equivalent heating unit
Q_r Heating rate due to radiation
T Temperature
V_{ni} Components of the winds perpendicular to the periphery of the pentagon
e Rate of re-evaporation of cloud droplets
$\bar{h}$ Regional averaged moist static energy
$\tilde{h}$ Environmental moist static energy
$\bar{h}_c$ Cloud moist static energy
$\bar{l}$ Mixing ratio of liquid water
p_0 Pressure at the ground level
p_t Pressure at the cloud top
$\bar{q}^*$ Regional averaged saturation mixing ratio
$\tilde{q}^*$ Environmental saturation mixing ratio
r Rate of precipitation
$\tilde{s}$ Environmental dry static energy
t Time
z Height
ε Rate of mass detrainment per unit pressure interval
ω_0 Vertical p-velocity at the ground level
∇ Horizontal gradient operator